Pramana – J. Phys., Vol. 39, No. 5, November 1992, pp. 529–539. © Printed in India.

f–α Spectrum of circle map

K M VALSAMMA, K BABU JOSEPH and G AMBIKA
Department of Physics, Cochin University of Science and Technology, Kochi 680 022, India

MS received 15 June 1992

Abstract. We present an analytic perturbative method for calculating $f(\alpha)$ and the generalized dimension D_q of the critical invariant circle of the polynomial circle map. The scaling behaviour is found to depend on z, the exponent defining the map. The asymptotic bounds of the scaling constants $\alpha(z)$ and $\delta(z)$ are verified analytically.

Keywords. Circle maps; universal constants; $f(\alpha)$ spectrum; generalized dimensions.

PACS Nos 05·45; 05·40; 47·20; 47·25

1. Introduction

The transition to chaos through the breaking of the quasiperiodic transition with two incommensurate frequencies has been studied before, from both theoretical and experimental points of view (Glazier *et al* 1989). The actual transition is usually preceded by mode-locking in which the ratio of the two frequencies is frozen at a rational value for a particular range of values of the parameter. Many features of this transition are described by maps of a circle onto itself (Feigenbaum *et al* 1982):

$$x_{i+1} = f(x_i) = x_i + \Omega - \frac{K}{2\pi}\sin(2\pi x_i) \tag{1}$$

where Ω is the ratio of the unperturbed frequencies and K the nonlinearity parameter. For $|K| < 1$ (subcritical), $f(x)$ is a simple invertible map (diffeomorphism) of a circle onto itself, whereas for $|K| = 0$, it is a simple linear map. Chaotic behaviour occurs only when $f(x)$ is noninvertible. The borderline between these two cases ($|K| = 1$) consists of critical circle mappings (homeomorphism) with one (usually cubic) inflection point (Feigenbaum 1978).

The dynamics of the map (1) is characterized by the rotation number

$$W = \lim_{n\to\infty} \frac{f^n(x) - x}{n}. \tag{2}$$

For the subcritical and critical maps, this number is independent of the initial point. The dependence $W(\Omega)$ is represented by the so called Devils' Staircase, wherein each rational $W = p/q$ is represented by an interval of Ω values (mode-locked values) and the observed motion is periodic with period q. The set of all these locked states has a full measure in the critical case (Swiatek 1988).

To study the quasiperiodic to chaos transition we focus our attention on a particular

quasiperiodic orbit, the one with inverse Golden Mean winding number. The continued fraction expansion of this winding number is given by the ratio of Fibonacci numbers $W_n = F_n/F_{n+1}$, where F_n is the nth Fibonacci number defined, $F_{n+1} = F_n + F_{n-1}$ for $n \geqslant 1$, with $F_0 = 0$ and $F_1 = 1$. The Golden Mean winding number is unique in that it is usually considered the best place to observe quasi periodicity because of its distance from rational approximants.

Renormalization Group (RG) studies of the circle map have revealed the existence of two scalling indices α and δ with values determined by the particular irrational number and the degree of inflection z. The generic equation for a circle map corresponding to a given z value has the polynomial form (Hu *et al* 1990)

$$x_{i+1} = f(x_i) = x_i + \Omega - x_i|2x_i|^{(z-1)/2} \tag{3}$$

with $x_i \in (-\frac{1}{2}, \frac{1}{2})$. For $z = 3$, this map gives the same α and δ values as for the sine circle map.

In this paper we try to extend the numerical results of Hu *et al* (1990) by examining the universal behaviour as well as multifractal nature of the attractor of the critical map in the quasiperiodic route, as the order of inflection z changes. For this purpose we use an analytic perturbation technique to solve the functional RG equations (Virendra Singh 1986; Ambika *et al* 1986) which has been used to compute the α and δ indices for the sine circle map (Valsamma and Ambika 1990) and to investigate its global characteristics. The generalized dimension D_q and the singularity strength $f(\alpha)$ are determined for different z values. The global behaviour of $z \to \infty$ is also discussed.

2. Perturbative evaluation of scaling constants for a polynomial circle map

We start with the RG equations for a circle map (Feigenbaum *et al* 1982):

$$g(x) = \alpha_{qp} g(g(x|\alpha_{qp}^2)) \tag{4}$$

$$g(x) = \alpha_{qp}^2 g(\alpha_{qp}^{-2}(g(x|\alpha_{qp})) \tag{5}$$

with $g(0) = 1$. These equations are formally the same as those for the sine circle map. In the perturbative approach these are replaced by infinite dimensional vector equations.

Let us expand $g(x)$ as a power series in $|x|^z$:

$$g(x) = 1 + \sum_{n=1}^{\infty} C_n |x|^{nz}. \tag{6}$$

Redefining the coefficients C_n by

$$C_n \alpha^n = S_n |\alpha|^{2z}. \tag{7}$$

Substituting (6) and (7) in (4) and equating the coefficients of $|x|^{nz}$ on both sides, the following relations are obtained:

$$\frac{1}{z} = \sum_{m=1}^{\infty} \frac{mS_m}{\alpha^{m-1}}, \tag{8}$$

$$\frac{1}{\alpha} - 1 - \alpha^{2z} \sum_{m=1}^{\infty} \frac{S_m}{\alpha^m} = 0, \tag{9}$$

$$S_n\left[1-\frac{1}{\alpha^{2z(n-1)}}\right]=\sum_{\ell\geqslant 2}^{n}\sum_{r\geqslant 1}^{\infty}\binom{\gamma Z}{\ell}\frac{S_r}{\alpha^{r-1}}$$

$$\times\sum_{m_1\geqslant 1,\ldots m_\ell\geqslant 1}\frac{S_{m_1}S_{m_2}\cdots S_{m_\ell}}{\alpha^{2z(n-\ell)}}S_{m_1+m_2+\cdots m_\ell,n}. \tag{10}$$

We may express the coefficients S_n as power series in $1/\alpha$:

$$S_n(\alpha)=\sum_{m=0}^{\infty}\frac{S_{nm}}{\alpha^m}. \tag{11}$$

Inserting (11) in (9) and (10), a set of relations for S_{nm} is obtained. Using the S_{nm} coefficients in (9) we get the equation for α as

$$\frac{1}{\alpha}-1=\alpha^{2z}\sum_{r=1}^{\infty}\sum_{m=0}^{\infty}\frac{S_{rm}}{\alpha^{r+m}}. \tag{12}$$

The determining equation for δ is

$$\alpha[g'(g(x)h(x))+hg(x)]=\delta h(\alpha^2 x). \tag{13}$$

Expanding $h(x)$ as a power series, as in the case of $g(x)$, we have

$$h(x)=1+\sum_{n=1}^{\infty}h_n|x|^{nz}. \tag{14}$$

Using (13), (6), (11) and (7) in (13) and equating coefficients of $|\alpha|^{nz}$ on both sides the following relations involving δ are obtained

$$\alpha\left[1+\sum_{m=1}^{\infty}h_m+\alpha^{2z}\sum_{m=1}^{\infty}\frac{mzS_m}{\alpha^m}\right]=\delta, \tag{15}$$

$$\alpha\left[\sum_{m\geqslant 1}^{\infty}\binom{mz}{1}h_m\frac{S_1}{\alpha}+\sum_{m\geqslant 1}^{\infty}2\binom{mz}{2}\frac{S_mS_1}{\alpha^m}|\alpha|^{2z-1}+h_1\sum_{m\geqslant 1}^{\infty}\binom{mz}{1}\frac{S_m}{\alpha^m}\right]=\delta h_1, \tag{16}$$

$$\alpha\left[\sum_{\ell\geqslant 1}^{n}\sum_{m\geqslant 1}^{\infty}\left(\binom{mz}{\ell}\frac{h_m}{\alpha^m}+(\ell+1)\binom{mz}{\ell+1}\left(\frac{S_m}{\alpha^{n-2z+m}}\right)\right)\sum_{m_1\geqslant 1,\ldots,m_\ell\geqslant 1}\right.$$

$$\times\frac{S_{m_1}S_{m_2}\cdots S_{m_\ell}\delta_{m_1+m_2+\ldots+m_\ell,n}}{\alpha^{2z(n-\ell)}}+\sum_{n'\geqslant 1}^{n-1}\sum_{n\geqslant 1}^{n-n'}\sum_{m\geqslant 1}^{\infty}h'_n(\ell+1)\binom{mz}{\ell+1}$$

$$\times\frac{S_m}{\alpha^{n-n'-2z+r}}\sum_{m_1\geqslant 1,\ldots,m_\ell\geqslant 1}\frac{S_{m_1}S_{m_2}\cdots S_{m_\ell}}{\alpha^{2z}(n-\ell)}\delta_{m_1+m_2+\ldots m_\ell,n}$$

$$\left.+h_n\sum_{m\geqslant 1}^{\infty}\frac{mzS_m}{\alpha^{m+(n-1)2z}}\right]=\delta h_n \tag{17}$$

(for $n=2,3,4\ldots$).

Equations (16) and (17) can be written in the form of a matrix eigenvalue equation, the elements of which are computed by means of equation (7) and S_{nm} coefficient.

The largest real eigenvalue gives δ value. The asymptotic series in (12) as well as in (17) can be replaced by Padé approximants [L/M] to ensure faster convergence (Ambika and Valsamma 1988). Figure 1 shows α_{qp} values thus obtained for different z values. The computed results along with their numerical values are given in table 1. The universal constants α and δ associated with quasiperiodic route have been computed numerically (Hu *et al* 1990). Agreement with numerically computed values is quite good except for $z = 2$.

A good replacement of the series by the Padé approximant is possible only if we locate the exact region of poles. We have studied the question whether this approach yields reasonable results in $z = 2$, by calculating the location of poles for each Padé approximated series. From this it is concluded that the deviation from numerical value for $z = 2$ is possibly due to the location of poles around the α_{qp} value. For high z values, the poles are found to shift as higher order approximants are considered. The computed δ values for varying z are given in table 2. α_{qp} is represented by a decreasing function while δ is an increasing function of z, as expected on the basis of the numerical findings (figure 2).

For a given z, the first few elements of S_{nm} are

$$S_{10} = \frac{1}{z}; \quad S_{11} = \frac{z-1}{z^2}; \quad S_{20} = \frac{z-1}{2z^2} \text{etc.} \tag{18}$$

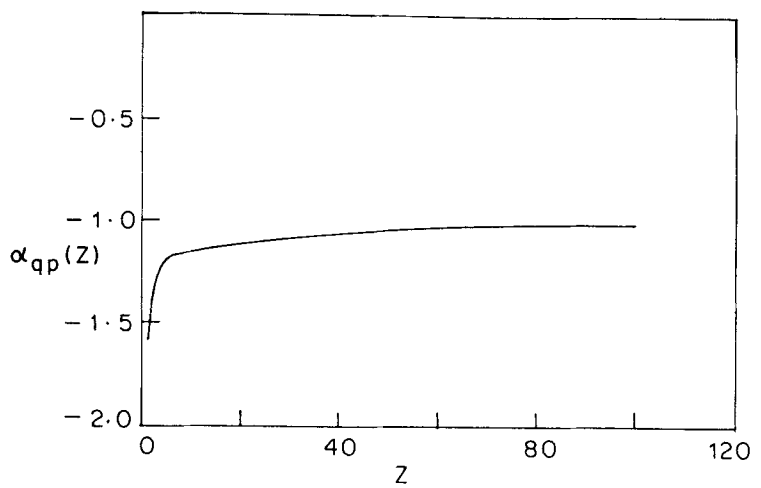

Figure 1. α_{qp} values for different z.

Table 1. Variation of α_{qp} values with z.

z	α_{qp} (calculated)	α Numerical value
1·1	−1·595027	—
2	−1·40421	−1·388
3	−1·28857	−1·288
4	−1·23110	−1·2314
5	−1·19024	−1·19
6	−1·1603	—
50	−1·0211	—
100	−1·01140	—

Table 2. Variation of δ values with z.

z	$\delta_{\text{calculated}}$	$\delta_{\text{numerical}}$
1·1	−1·60804	—
2	−2·706712	−2·707
3	−2·83350	−2·833
4	−2·94576	−2·946
5	−3·04017	−3·04
6	−3·1919	—
50	−3·98979	—
100	−4·01414	—

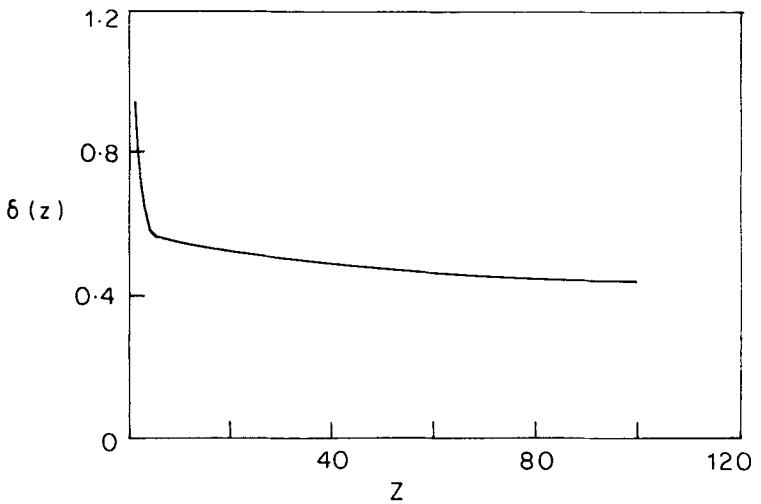

Figure 2. $\delta(z)$ as a function of degree of inflection z.

with this set of S_{nm} coefficients, the function $g(x)$ is obtained in the form:

$$g(x) = 1 + \alpha^{2z}\left(\frac{1}{z\alpha_{qp}} - \frac{z-1}{z^2\alpha_{qp}^2}x^z + \frac{z-1}{2z^2\alpha_{qp}^2}x^{2z} + \ldots\right) \tag{19}$$

The behaviour of $g(x)$ in the interval $(0, 1)$ is sketched in figure 3. As is evident, the curves for distinct z values are very close for small x, and are well separated for large x.

3. *f–α* Spectrum of circle maps

Circle maps possess unusual scaling properties at the transition $k = 1$. The corresponding behaviour is characterized by the universal function $g(x)$. The attractor consists of a set of points that are found to follow the construction of a Cantor set. At each stage of construction, the probabilities P_i are almost equal while the lengths ℓ_i of the subset are different. Using (4) the first few iterates of $g(x)$ starting from $x_0 = 0$, are:

$$x_1 = 1, \quad x_2 = \frac{1}{\alpha_{qp}}, \quad x_3 = g\left(\frac{1}{\alpha}\right)_{qp} \text{ and } x_4 = \frac{1}{\alpha}g(\alpha)_{qp} \tag{20}$$

which after rescaling fall in the interval (0,1) so that

$$x'_1 = 1, \quad x'_2 = 0,$$

$$x'_3 = \frac{g(1/\alpha_{qp}) - (1/\alpha_{qp})}{1 - (1/\alpha_{qp})}$$

and

$$x'_4 = \frac{(1/\alpha)g(\alpha_{qp}) - (1/\alpha_{qp})}{1 - (1/\alpha_{qp})}. \tag{21}$$

The rescaled subsets are

$$S_1 = \frac{1}{x'_1 - x'_3}, \quad S_2 = \frac{1}{x'_4 - x'_3} \tag{22}$$

where the lengths ℓ'_i are given by

$$\ell'_i = x'_1 - x'_3, \quad \ell'_2 = x'_4 - x'_2. \tag{23}$$

Since the probabilities P_i are nearly equal for those sets we might expect that

$$S_1 + S_2 = 2^q \tag{24}$$

as the equation determining the partition function τ. But actual calculation shows that far better agreement with numerical results is obtained with the Golden Mean number

$$\rho = \frac{\sqrt{5} - 1}{2}$$

in place of 2 in (24).

For an asymptotically recursive structure, this partition is of order unity only when

$$\tau = (q - 1)D_q \tag{25}$$

where D_q defines a set of generalized dimensions, of which D_0 is the Hausdorff dimension, D_1 the information and D_2 the correlation dimension. The $f(\alpha)$ spectrum is defined by a Legendre transformation of $\tau(q)$:

$$\alpha(q) = \frac{\partial \tau}{\partial q}, \tag{26}$$

$$f(q) = q\alpha(q) - \tau. \tag{27}$$

For any specific q, equation (24) is solved for $\tau(q)$ by a root finding procedure

$$\alpha = \frac{\partial \tau}{\partial q} = \frac{\rho^q \ln \rho}{S_1^\tau \ln S_1 + S_2^\tau \ln S_2}. \tag{28}$$

The f–α plot is computed using (27). The D_q versus q curves for a few z values are shown in figure 4. It is clear that as z increases the change in D_q over the interval $(-q, q)$ becomes sharp. The D_q values tend to converge on the $+q$ side while they are far apart on the $-q$ side. Figure 5 depicts the continuous variation of D_q with

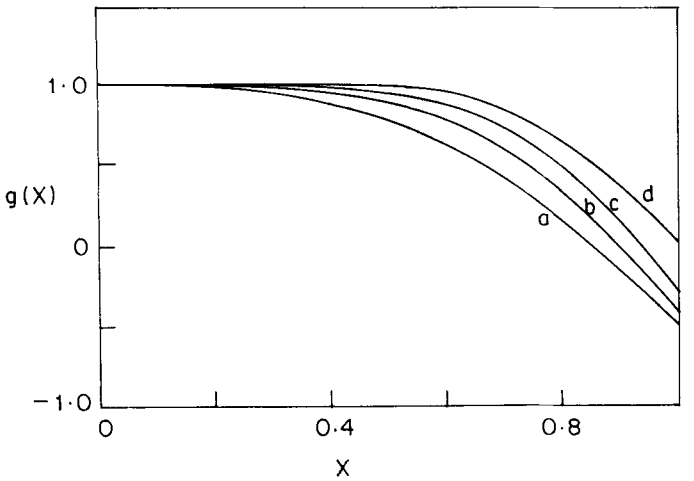

Figure 3. The universal function $g(x)$ computed using (19) for a) $z = 2$, b) $z = 3$, c) $z = 4$ and d) $z = 5$.

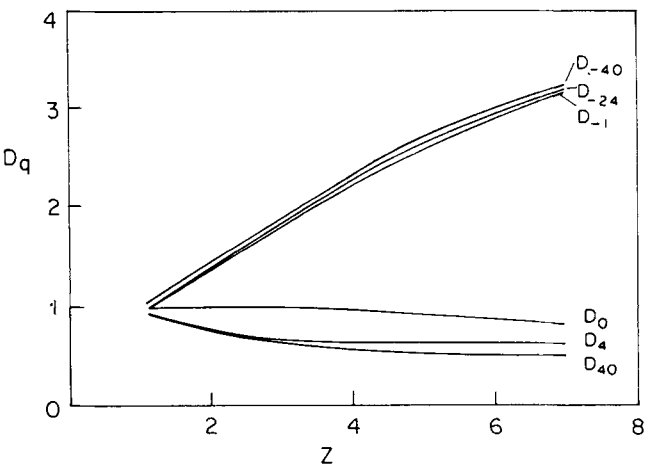

Figure 4. The dependence of fractal dimensions D_q on degree of inflection z.

z. D_q values spread over a wide range, and the values are asymmetric about D_0. For large q values D_q gets closer the closer. The D_q values are very close for both positive and negative q values.

Using (27) and (28) we have calculated the f–α values for specific z values. The f–α curves are seen to crowd near $D_{+\infty}$ region for large z but they are distributed uniformly over the curve for small z (figure 6). Moreover, the $D_{+\infty}$ values are not much different for different z values. The $D_{-\infty}$ values, however, differ considerably. For very large z (say 50 and 100) shown separately in figure 7 the f–α curves are flat at the top portion with the exponents clustering about the flat portion. It can be seen from the graph that, as z increases, the points on the attractor exhibit a tendency towards uniform distribution, avoiding the rarefied and concentrated regions.

The end-points of the f–α curves can be determined by the local scaling exponents,

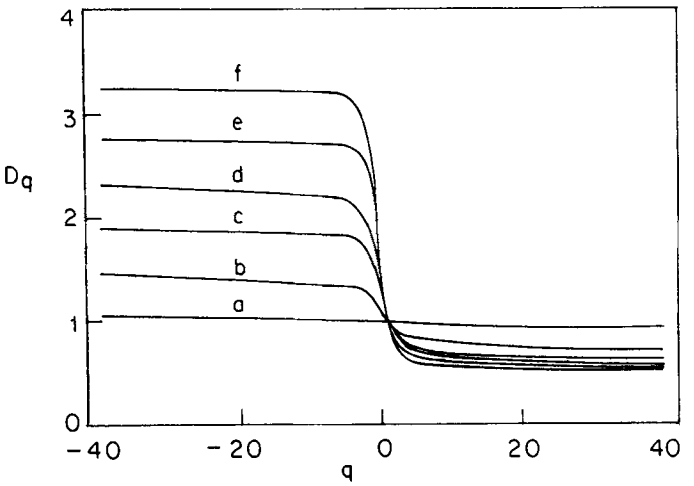

Figure 5. Plot of fractal dimension D_q vs q for typical z values: a) $z = 1{\cdot}1$, b) $z = 2$, c) $z = 3$, d) $z = 4$, e) $z = 5$ and f) $z = 6$.

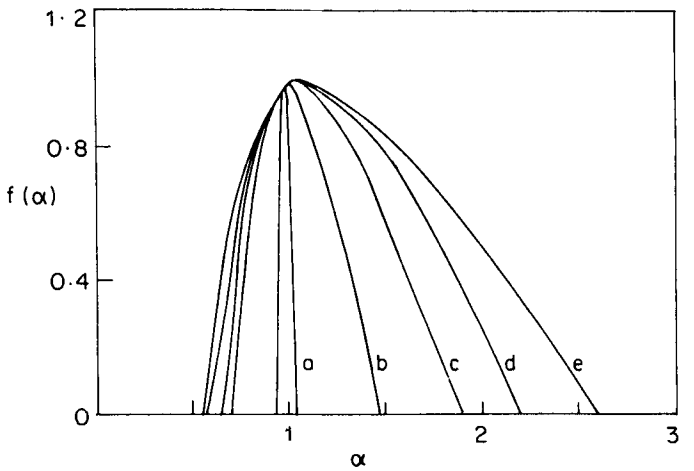

Figure 6. The f against α curve for typical z values: a) $z = 1{\cdot}1$, b) $z = 2$, c) $z = 3$, d) $z = 4$, e) and $z = 5$.

which, for quasi-periodicity, are given by (Halsey *et al* 1986)

$$D_{\infty} = \frac{\ln \rho}{\ln \alpha_{qp}^{-z}}$$

and

$$D_{-\infty} = \frac{\ln \rho}{\ln \alpha_{qp}^{-1}} \tag{29}$$

There is excellent agreement between the $D_{\pm\infty}$ values obtained from the f–α curves with those given by (29). The results obtained are given in table 3. For very large z values, the computed $D_{\pm\infty}$ values are used to complete the f–α curve. The variation of $D_{\pm\infty}$ with z is shown in figures 8 and 9. We conclude that $D_{-\infty}$ is a monotone

Table 3. $D_{\pm\infty}$ values computed graphically. (Numerical values are given for comparison).

	$D_{+\infty}$		$D_{-\infty}$	
z	Calculation	Graph	Calculation	Graph
1·1	0·936975	0·940	1·030673	1·04
2	0·708985	0·706	1·466051	1·47
3	0·632533	0·640	1·898241	1·80
4	0·578794	0·573	2·314572	2·40
5	0·552625	0·552	2·763125	2·76
50	0·460973	0·458	22·11329	—
100	0·4399173	0·440	43·98728	—

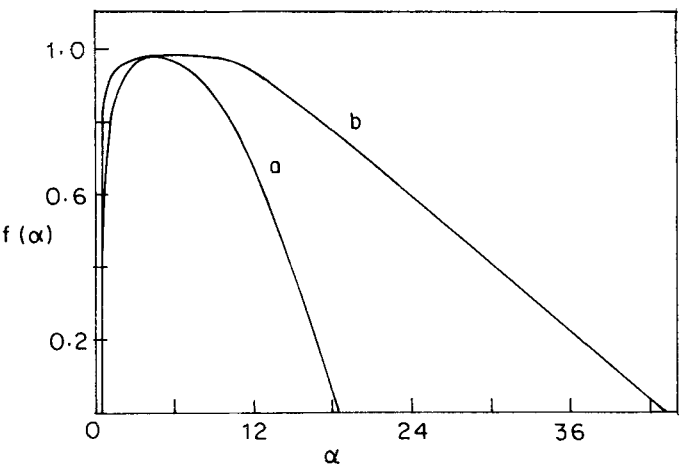

Figure 7. f–α curves for a) $z = 50$ and b) $z = 100$.

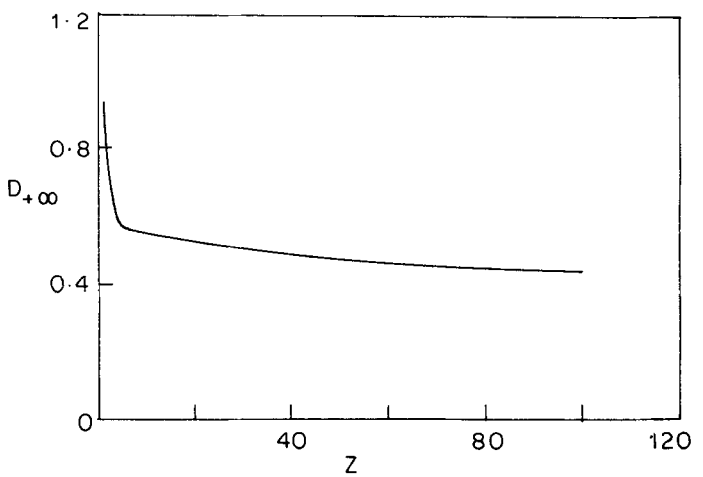

Figure 8. Variation of $D_{+\infty}(\alpha_{min})$ with z.

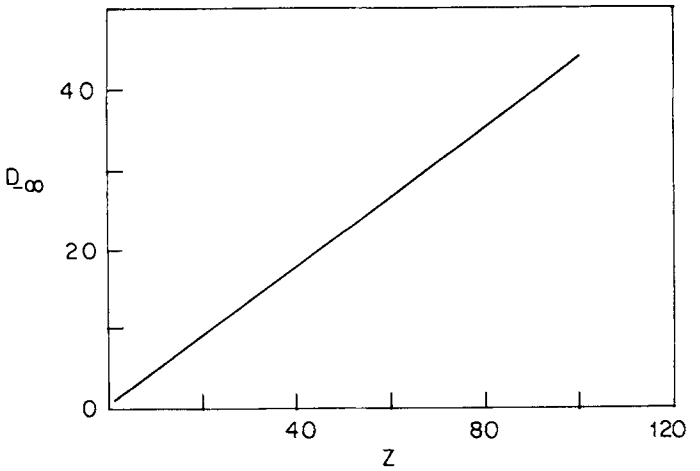

Figure 9. Variation of $D_{-\infty}(\alpha_{max})$ with z.

increasing function while D_∞ is a decreasing one. Demanding that (29) implies

$$\alpha_{max} = Z\alpha_{min} \tag{30}$$

one obtains the same result from the graph, which is true for any z value. On the basis of this relation, from the experimentally observed f–α curve, one can identify the map of relevance for any z. The important fact is that the same relation holds also for one-dimensional maps (Stavans *et al* 1985). All these seem to suggest that the degree of inflection z can serve as the universality index in circle maps too.

4. Summary and discussion

We have addressed the behaviour of the singularity spectrum for polynominal circle maps. The general fremework used is an analytic perturbative scheme coupled with Padé technique. It is observed that for the polynomial circle map $\alpha(z)$ is a monotone decreasing function of z while $\delta(z)$ is an increasing one. The asymptotic limit of $\alpha(z)$ is -1 while that of $\delta(z)$ is -4 in agreement with numerical data. These bounds are known to hold for the period-doubling route as well.

Being purely analytic, the method used here avoids lengthy computations. With the help of (30) it is possible in principle to determine the universality class of a given map. It is to be remarked that the same relation holds for 1–d maps. Thus the perturbative approach coupled with Padé technique has the advantage that an analytically determined universal function $g(x)$ is employed with the accuracy being dependent on the number of terms in $g(x)$. The method yields good values using a few steps.

References

Ambika G and Babu Joseph K 1986 *Pramana – J. Phys.* **26** 465
Ambika G and Valsamma K M 1988 *Pramana – J. Phys.* **30** 501

Feigenbaum M J 1978 *J. Stat. Phys.* **19** 25
Feigenbaum M J, Kadanoff L P and Shenker S J 1982 *Physica* **5D** 370
Glazier J A, Jensen M H, Libchaber A and Stavans J 1986 *Phys. Rev.* **A34** 1621
Halsey T C, Jensen M H, Kadanoff L P, Proccacia I and Shraiman B I 1986 *Phys. Rev.* **A40** 1141
Hu B, Valinia A and Piro O 1990 *Phys. Lett.* **A144** 7
Stavans J, Heslot F and Libchaber A 1985 *Phys. Rev. Lett.* **55** 596
Swiatek G 1988 *Comm. Math. Phys.* **119** 109
Valsamma K M and Ambika G 1990 *Phys. Scr.* **42** 19
Virendra Singh 1985 *Pramana – J. Phys.* **24** 31